

**Advanced Materials
Science and Technology
ICAMST 2013**

Edited by
Kuwat Triyana, Khairurrijal, Risa Suryana,
Heru Susanto and Sutikno

Advanced Materials Science and Technology

ICAMST 2013

Edited by
Kuwat Triyana
Khairurrijal
Risa Suryana
Heru Susanto
Sutikno

Advanced Materials Science and Technology

ICAMST 2013

Selected, peer reviewed papers from the
2013 International Conference on
Advanced Materials Science and Technology
(ICAMST 2013),
September 17-18, 2013, Yogyakarta, Indonesia

Edited by

**Kuwat Triyana, Khairurrijal, Risa Suryana,
Heru Susanto and Sutikno**



Copyright © 2014 Trans Tech Publications Ltd, Switzerland

All rights reserved. No part of the contents of this publication may be reproduced or transmitted in any form or by any means without the written permission of the publisher.

Trans Tech Publications Ltd
Kreuzstrasse 10
CH-8635 Durnten-Zurich
Switzerland
<http://www.ttp.net>

Volume 896 of
Advanced Materials Research
ISSN print 1022-6680
ISSN cd 1022-6680
ISSN web 1662-8985

Full text available online at <http://www.scientific.net>

Distributed worldwide by

Trans Tech Publications Ltd
Kreuzstrasse 10
CH-8635 Durnten-Zurich
Switzerland

Fax: +41 (44) 922 10 33
e-mail: sales@ttp.net

and in the Americas by

Trans Tech Publications Inc.
PO Box 699, May Street
Enfield, NH 03748
USA

Phone: +1 (603) 632-7377
Fax: +1 (603) 632-5611
e-mail: sales-usa@ttp.net

printed in Germany

Table of Contents

Preface	v
Conference Organizers	vi

Chapter 1: Nanofibers and Membranes

The Role and Prospect of Nanomaterials in Polymeric Membrane for Water and Wastewater Treatment: A State-of-the-Art Overview A.F. Ismail and P.S. Goh.....	3
Synthesis of Low Fouling Porous Polymeric Membranes H. Susanto, D.P. Julyanti and A. Roihatin.....	7
Mass Production of Stacked Styrofoam Nanofibers Using a Multinozzle and Drum Collector Electrospinning System M.M. Munir, A.Y. Nuryantini, Iskandar, T. Suciati and Khairurrijal.....	20
Transparent and Conductive Fluorinated-Tin Oxide Prepared by Atmospheric Deposition Technique A. Purwanto.....	24
Gas Sensing Using Static and Dynamic Modes Piezoresistive Microcantilever R. Nuryadi, L. Aprilia, N. Aisah and D. Hartanto.....	29
One-Step Fabrication of Short Nanofibers by Electrospinning: Effect of Needle Size on Nanofiber Length I.W. Fathona, Khairurrijal and A. Yabuki.....	33
Carbon Dioxide Permeation Characteristics in Asymmetric Polysulfone Hollow Fiber Membrane: Effect of Constant Heating and Progressive Heating M.A. Bin Azhari, N. Binti Omar, N. Binti Mustaffa and A.F. Ismail.....	37
Electrospinning of Poly(vinyl alcohol)/Chitosan via Multi-Nozzle Spinneret and Drum Collector A.Y. Nuryantini, M.M. Munir, M.P. Ekaputra, T. Suciati and Khairurrijal.....	41
A Simple Way of Producing Nano Anatase TiO₂ in Polyvinyl Alcohol Fibers Harsojo, K. Triyana and H. Sosiati.....	45
The Crystal Structure, Conductivity Character and Ionic Migration of Samarium Doped-Ceria (SDC) and its Composite with Sodium Carbonate F. Rahmawati, D.G. Syarif, P.P. Paramita and E. Heraldly.....	49
Preparation of Sulfonate Grafted Silica/Chitosan-Based Proton Exchange Membrane Z.M. Putrie and H. Setyawan.....	54
Synthesis and Characterization of Solid Polymer Electrolyte from <i>N</i>-Succinyl Chitosan and Lithium Perchlorate I. Fauzi, I.M. Arcana and D. Wahyuningrum.....	58
Epoxidised Natural Rubber Based Polymer Electrolyte Systems for Electrochemical Device Applications R. Idris and N.H. Bujang.....	62
Eggs Shell Membrane as Natural Separator for Supercapacitor Applications E. Taer, Sugianto, M.A. Sumantre, R. Taslim, Iwantono, D. Dahlan and M. Deraman.....	66
Titania Coated Ceramic Membrane from Clay and Muntilan Sand for Wastewater Filter Application Masturi, E. Sustini, Khairurrijal and A. Mikrajuddin.....	70

Utilization of Fly Ash as Ceramic Support Mixture for the Synthesis of Zeolite Pervaporation Membrane	
B. Alfijan and H. Susanto.....	74
Synthesis and Characterization of Nanostructured Tungsten Oxide by Hard Template Method	
T. Hongo, Y. Usami and A. Yamazaki	78
Chapter 2: Nanoparticles and Powders	
Excited-State Proton Transfer in Fluorescent Photoactive Yellow Protein Containing 7-Hydroxycoumarin	
D. Novitasari, H. Kamikubo, Y. Yamazaki, M. Yamaguchi and M. Kataoka.....	85
Effect of Heating Time on Atrazine-Based MIP Materials Synthesized via the Cooling-Heating Method	
I. Royani, Widayani, A. Mikrajuddin and Khairurrijal	89
Preparation of Orange Peel Based Activated Carbons as Cathodes in Lithium Ion Capacitors	
A.A. Arie, H. Kristianto, I. Suharto, M. Halim and J.K. Lee.....	95
Synthesis of Fe₂O₃/C Nanocomposite Using Microwave Assisted Calcination Method	
A.P. Swardhani, F. Iskandar, A. Mikrajuddin and Khairurrijal	100
Magnetic CuFe₂O₄ Nanoparticles for Adsorption of Cr(VI) from Aqueous Solution	
P.L. Hariani and F. Riyanti	104
Optical Properties of Zn-Doped CeO₂ Nanoparticles as a Function of Zn Content	
I. Nurhasanah, H. Sutanto and R. Futikhaningtyas	108
Chelating Agent Role in Synthesizing Cerate-Zirconate Powder by a Sol-Gel Method	
N. Osman, N.A. Abdullah and S. Hasan	112
Influence of Ionic Surfactants under Ultrasonic Irradiation to Reduce the Particle Size of Mechanically Alloyed La_{1-x}Sr_x Fe_{0.5}Mn_{0.25}Ti_{0.25}O₃ Powders	
M.A.E. Hafizah, A. Manaf and B. Soegijono	116
Covalent Functionalization of Amino Group onto Carbon-Based Magnetic Nanoparticles Using Pulsed-Powder Explosion Technique	
T.E. Saraswati, S. Tsumura and M. Nagatsu.....	122
Magnetic Properties and Microstructures of Polyethylene Glycol (PEG)-Coated Cobalt Ferrite (CoFe₂O₄) Nanoparticles Synthesized by Coprecipitation Method	
E. Suharyadi, E.A. Setiadi, N. Shabrina, T. Kato and S. Iwata.....	126
Copper-Zinc-Titania Nanocomposite as Catalyst for CO₂ Photo-Reduction: A Surface Deactivation Study	
O. Zuas, Y.K. Krisnandi, W. Wibowo, J.S. Kim and J. Gunlazuardi	134
The Highly Active Photocatalyst of Silver Orthophosphate under Visible Light Irradiation for Phenol Oxidation	
U. Sulaeman, I.R. Nisa, A. Riapanitra, P. Iswanto, S. Yin and T. Sato	141
Treatment of Coal Stockpile Wastewater by Electrocoagulation using Aluminum Electrodes	
Rusdianasari, Y. Bow and A. Taqwa	145
Preparation of Activated Carbons from Coconuts Shell for Pb (II) Adsorption	
E. Yusmartini, D. Setiabudidaya, Ridwan, Marsi and Faizal.....	149
Preparation of Sulfated Zirconia Using Modified Sol Gel Method	
A. Kristiani, K.C. Sembiring, F. Aulia, J.A. Laksmono, S. Tursiloadi and H. Abimanyu	153

Enrichment of Indonesian Low Rank Coal's Surface Oxygen Compounds (SOCs) Using Hydrogen Peroxide and its Adsorptive Properties G. Yuliani, I. Noviyana and A. Setiabudi	159
Characteristics of Water-ZrO₂ Nanofluids with Different pH Utilizing Local ZrO₂ Nanoparticle Prepared by Precipitation Method D.G. Syarif	163
Corrosion of Carbon Steel in Nanofluid Containing ZrO₂ Nanoparticle at Different Temperature D.H. Prajitno and D.G. Syarif	168

Chapter 3: Thick and Thin Films

Contact Formation at Interface of LSCO BCZY LSCO Symmetrical Cell: Effect of LSCO to PVP Ratio A.A. Samat, S.A. Safri, D. Samsudin, W.S. Jaafar and N. Osman	175
Preparation of Activated Carbon Monolith Electrodes from Sugarcane Bagasse by Physical and Physical-Chemical Activation Process for Supercapacitor Application E. Taer, Iwantono, S.T. Manik, R. Taslim, D. Dahlan and M. Deraman	179
The Effect of Paste Preparation and Annealing Temperature of ZnO Photoelectrode to Dye-Sensitized Solar Cells (DSSC) Performance A. Syukron, R.A. Wahyuono, D. Sawitri and D.D. Risanti	183
Utilization of Natural Porphyrin Thin Films as a Photosensitizer for Photodetectors Utari, A. Heru Wibowo, B. Purnama and K. Abraha	187
Effect of Growth Temperature on Cobalt-Doped TiO₂ Thin Films Deposited on Si (100) Substrate by MOCVD Technique A. Saripudin, H. Saragih, Khairurrijal, T. Winata and P. Arifin	192
Fabrication of Aluminum Doped Silica Preform Using MCVD and Solution Doping Technique: Soot Analyses and Solution Concentration Effect S.M. Aljamimi, Z. Yusoff, H.A. Abdul-Rashid, K.M.S. Anuar, S.Z. Muhamad Yassin, M.I. Zulkifli, S. Hanif and N. Tamchek	197
The Influence of Mn/Ga Solution Mole Fraction on the Solid Composition and Microstructure of GaN:Mn Thin Film Deposited on Silicon Substrate by Spin Coating Technique H. Sutanto, I. Nurhasanah, I. Istadi and Priyono	203
Grain Size Analysis on Ba_{0.65}Sr_{0.35}TiO₃ Thin Films Using Design of Experiment V. Retnasamy, Z. Sauli, R. Vairavan, S. Tanisellass, M.H. Ab Aziz, P. Ehkan and F.A.A. Fuad	211
Fabrication and Characterization of Stacked Self-Assembled In_{0.5}Ga_{0.5}As/GaAs Quantum Dots Grown by MOCVD D. Aryanto, Z. Othaman and A.K. Ismail	215
Er₂O₃-Al₂O₃ Doped Silica Preform Prepared by MCVD-Chelate Vapor Phase Delivery Technique K.M.S. Anuar, S.Z. Muhd-Yasin, M.I. Zulkifli, S. Hanif, A. Yusoff, S.M. Aljamimi, H.T. Zubair, Z. Yusoff, H.A. Abdul-Rashid and N. Tamchek	219
The Effect of Variation Concentration Nd³⁺ Ions on Physical and Optical Properties of TZBN Glass E. Nurliana, Riyatun and L. Rahmasari	225
Effects of Iron Dopants on Barium Strontium Titanate (Ba_{0.8}Sr_{0.2}TiO₃) Thin Films R.T. Setyadhani, A. Jamaludin and Y. Iriani	229
Wettability Study Using O₂ and Ar RIE Gas Treatment on Aluminium Surface V. Retnasamy, Z. Sauli, M. Palianysamy, S. Tanisellass, P. Ehkan and F.A.A. Fuad	233

Room-Temperature Deposition of ZnO Thin Films by Using DC Magnetron Sputtering P. Marwoto, Sulhadi, Sugianto, D. Aryanto, E. Wibowo and K. Wahyuningsih.....	237
Defects Induced by Reactive Ion Etching in Ge Substrate Kusumandari, N. Taoka, W. Takeuchi, M. Sakashita, O. Nakatsuka and S. Zaima	241
Effect of Electrolyte Composition on Corrosion Resistance in Nickel Plating Process for Coating Bonded Magnet PrFeB C. Kurniawan, H.M.A. Sholihat, K.A.Z. Thosin, Muljadi and P. Sardjono.....	245
Effects of Sputtering Coating Factors on Elastic Modulus of MoN Coatings P. Srisattayakul, C. Saikaew, A. Wisitsoraat and N. Intanon.....	249
Effect of Anodizing in Surface Finishing on Speed Boat Impeller Made of Aluminum S. Soekrisno and B. Anggoro.....	253
Chapter 4: Biomaterials	
Biomimetic Creation of Surfaces on Porous Titanium for Biomedical Applications K. Mediaswanti, C. Wen, E.P. Ivanova, F. Malherbe, C.C. Berndt, V.T.H. Pham and J. Wang.....	259
Production and Characterization of Biodegradable Plastics Based on Starch of <i>Artocarpus heterophyllus</i> Lam Seeds Sutikno, P. Marwoto and A. Dian Puspita	263
Characteristics of Mg-Ca-Zn Alloy Metallic Foam Based on Mg-Zn-CaH₂ System I. Kartika, Y.N. Thaha, F. Pramuji Lestari and B. Sriyono.....	267
The Effect of Repeated Impingement on UHMWPE Material in Artificial Hip Joint during Salat Activities J. Jamari, R. Ismail, E. Saputra, S. Sugiyanto and I.B. Anwar	272
Simple and Easy Method to Synthesize Chicken Eggshell Based Hydroxyapatite S. Tri Wahyudi, S. Utami Dewi, A. Anggraeni, K. Dahlan, Akhmaloka, M. Ali Zulfikar and R. Hertadi.....	276
Synthesis of Chitosan-Gold Nanoparticles for Drug Delivery H. Yazid, A.M. Yassin, A.Z. Ruslan, S.H. Alias, R. Adnan and A.M. Md Jani.....	280
Synthesis of Hydroxyapatite Nanoparticle from Tutut (<i>Bellamyia javanica</i>) Shells by Using Precipitation Method for Artificial Bone Engineering L. Herawaty, E. Rohaeti, Charlena and S.G. Sukaryo	284
Adsorption of Lead Ions onto Citric Acid Modified Rubber (<i>Hevea brasiliensis</i>) Leaves S. Ibrahim, M.A.K. Megat Hanafiah and F. Fadzil.....	288
Effect of Deacetylation on Characterization of pH Stimulus Responsive Chitosan-Acrylamide Hydrogels Using Radiation K.T. Basuki, D. Swantomo, Sigit and K. Megasari	292
Synthesis of Smart Biodegradable Hydrogels Cellulose-Acrylamide Using Radiation as Controlled Release Fertilizers D. Swantomo, Rochmadi, K.T. Basuki and R. Sudiyo	296
Structural Studies of 1,3:2,4-Dibenzylidene Sorbitol Gels H. Takeno and Y. Kuribayashi.....	300
Effects of Surface Treatments on Nata de Cassava on the Tensile Strength and Morphology of Bacterial Cellulose Sheet D. Cahyandari and H.S. Budi Rohardjo	305
Impact and Thermal Properties of Unsaturated Polyester (UPR) Composites Filled with Empty Fruit Bunch Palm Oil (EFBPO) and Cellulose E. Surya, Michael, Halimatuddahlia and Maulida.....	310

Biodegradation of Low Density Polyethylene (LDPE) Composite Filled with Cellulose and Cellulose Acetate	
Halimatuddahlia and A.M. Rambe	314
The Treated Rice Straw as Potentially Feedstock of Wood and Rice Straw Fiber Blend for Pulp and Paper Making Industry	
A.L. Juwono and H. Subawi	318
Experimental Studies of Thermo-Induced Mechanical Effects in the Main-Chain Liquid Crystal Elastomers	
Supardi, Harsojo and Y. Yusuf	322
Characterization of Photo Biocomposites for Application in Biomedical Materials	
J. Triyono, A.E. Tontowi, W. Siswomihardjo and Rochmadi	327
Study on Ginger Extract Performance as Corrosion Inhibitor in Acid and Neutral Environments	
B.A. Kurniawan, A. Pradana, Sulistijono and Sutarsis	331
Comparison between Slip Casting and Cold Isostatic Pressing for the Fabrication of Nanostructured Zirconia	
N.F. Amat, A. Muchtar, N. Yahaya, M.J. Ghazali and C.C. Hao	335

Chapter 5: Electronic Materials

Fabrication of Silver Nanoparticles and its Films and their Characterization of Structure and Electrical Conductivity	
M. Diantoro, A.F. Chasanah, Nasikhudin, N. Mufti and A. Fuad	341
Crystallographic and Electrical Properties of Barium Zirconium Titanate Doped by Indium and Lanthanum	
S.R. Adnan, M. Hikam and E. Rizky	347
Ohmic Contact in P-HEMT Wafer Using Metallization with Ge/Au/Ni/Au	
A. Dolah, M.A. Abd Hamid, M. Deraman, A. Yusof, N.A. Ngah and N.F.I. Muhammad	351
Possible Existence of the Stripe Correlations in Electron-Doped Superconducting Cuprates $\text{Eu}_{1.85}\text{Ce}_{0.15}\text{Cu}_{1-y}\text{Ni}_y\text{O}_{4+a-\delta}$ Studied by Muon-Spin-Relaxation	
Risdiana, L. Safriani, W.A. Somantri, T. Saragi, T. Adachi, I. Kawasaki, I. Watanabe and Y. Koike	354
Fabrication and Characterization of Ferroelectric Thin Film $\text{Ba}_x\text{Sr}_{1-x}\text{TiO}_3$ for Application in Light Intensity Detector	
A. Jamaluddin, E. Susilowati, S. Budiawanti and Y. Iriani	358
A Theoretical Study on Electron Tunneling Current in Isotropic High-κ Dielectric Stack-Based MOS Capacitors with Charge Trapping	
F.A. Noor, Khairiah, A. Mikrajuddin and Khairurrijal	363
Modeling of Drain Current in Armchair Graphene Nanoribbon Field Effect Transistor Using Transfer Matrix Method	
E. Suhendi, F.A. Noor, N. Kurniasih and Khairurrijal	367
A Theoretical Model of Band-to-Band Tunneling Current in an Armchair Graphene Nanoribbon Tunnel Field-Effect Transistor	
C.S.P. Bimo, F.A. Noor, M. Abdullah and Khairurrijal	371
Determination of Thin Film $\text{Ba}_{0.5}\text{Sr}_{0.5}\text{TiO}_3$ Ferroelectric Effective Mass from I-V Characteristics Calculation Using Transfer Matrix Method	
L. Hasanah, I. Hamidah, A. Hamdani, B. Mulyanti, D. Rusdiana and H. Yuwono	375

Chapter 6: Magnetic Materials

Thermal Analysis and Magnetic Properties of Lanthanum Barium Manganite Perovskite P. Sardjono and W. Ari Adi	381
Magnetoelectric Coupling Phenomena Based on the Changes of Magnetic Properties in Multiferroic Nanocomposite BaTiO₃-BaFe₁₂O₁₉ D. Suastiyanti, B. Soegijono and M. Hikam	385
Microstructural Studies of (Ba_{0.7}Sr_{0.3}Fe₁₂O₁₉)_{1-x} - (Ba_{0.7}Sr_{0.3}TiO₃)_x with x = 0.2, x = 0.5 and x = 0.8 Composite System by Mechanical Alloying Process Novizal, A. Manaf and P. Sardjono	391
Modeling of Magnetorheological Damper Using Back Propagation Neural Network Ubaidillah, G. Priyandoko, M. Nizam and I. Yahya	396
Microstructural and Magnetic Properties of Ti²⁺-Mn⁴⁺ Substituted Barium Hexaferrite M. Manawan, A. Manaf, B. Soegijono and A. Yudi	401
The Influence of Ni-Doping on Structure and Magnetic Properties of La_{0.67}Ba_{0.33}MnO₃ S.S. Ahmiatri, A. Manaf and B. Kurniawan	406
Micromagnetic Study on the Dynamic Susceptibility Spectra of Square-Patterned Ferromagnets D. Djuhana, J.A. Kadir, A.T. Widodo and D.H. Kim	410
Micromagnetic Simulation on Ground State Domain Structures of Barium Hexaferrite (BaFe₁₂O₁₉) D. Djuhana, D.C.C. Oktri and D.H. Kim	414
Magnetic Properties and Reflection Loss Characteristic of Mn-Ti Substituted Barium-Strontium Hexaferrite V.V.R. Repi, A. Manaf and B. Soegiono	418
Analysis of Structural and Microstructure of Lanthanum Ferrite by Modifying Iron Sand for Microwave Absorber Material Application N. Taufiqu Rochman and W. Ari Adi	423
Characterization of Single Phase of La_{0.8}Ba_{0.2}Fe_{0.3}Mn_{0.35}Ti_{0.35}O₃ Nanoparticles as Microwave Absorbers A. Manaf and W. Ari Adi	428
Magnetic Properties of Coring Samples from Aceh Basin West Off Sumatera Island E.Z. Gaffar	434
Microwave Properties of Composite Ba_{0.5}Sr_{0.5}Fe_{11.7}Mn_{0.15}Ti_{0.15}O₁₉/La_{0.7}Ba_{0.3}MnO₃ Material V.V.R. Repi, A. Manaf and B. Soegiono	440
Experiment Using a Magnetically Controlled Ferrofluid Flow in a Flatplate Laminar Flow System Y.H. Fan, L.Y. Lou and Y.M. Chen	444

Chapter 7: Optical Materials

Anode Buffer for Organic Devices Composed of Gold Nanoparticles Prepared by Ark Plasma Deposition D. Wang, N. Yukitake and K. Fujita	451
A Simple Optimization of Triple-Junction Solar Cell nc-Si:H/a-Si:H/a-SiGe:H Using Computer Modeling and Robust Design T. Abuzairi and N. Raden Poespawati	455

Detailed Analysis of Shallow and Heavily-Doped Emitters for Al-BSF Bifacial Solar Cells S. Sepeai, S.H. Zaidi, M.Y. Sulaiman, K. Sopian, M.A. Ibrahim, M.K.M. Desa and M.D. Norizam.....	459
Microwave-Assisted Solid State Synthesis of Red-Emitting BCNO Phosphor and its Characteristics B.W. Nuryadin, E.C. Septia, F. Iskandar, T. Ogi, K. Okuyama, A. Mikrajuddin and Khairurrijal	464
Synthesized 2,4,5-Triphenylimidazole as Precursor of Organic Light Emitting Diode (OLED) Material I.B. Rachman and D. Wahyuningrum	468
Preliminary Study on the Photovoltaic and Impedance Characteristics of Dye Sensitized Solar Cell (DSSC) using Polymer Gel Electrolyte W.S. Arsyad, H. Pujiarti, P. Wulandari, Herman and R. Hidayat.....	472
Charge Carrier Dynamics of Active Material Solar Cell P3HT:ZnO Nanoparticles Studied by Muon Spin Relaxation (μSR) L. Safriani, Risdiana, A. Bahtiar, A. Aprilia, R.E. Siregar, R. Hidayat, T.P.I. Saragi, I. Kawasaki and I. Watanabe.....	477
Influence of Mass Ratio of Aquadest and TTIP on the Synthesis of TiO₂ Nanoparticles to Improve the Performance of DSSC with Beta-Carotene as Sensitizer N. Ardhani, A. Supriyanto, A.H. Yuwono and R. Suryana	481
Sol-Gel Derived ZnO Nanorod Templated TiO₂ Nanotube Synthesis for Natural Dye Sensitized Solar Cell I. Kartini, Evana, Sutarno and Chotimah	485
Organic-Inorganic Solar Cell Based on Sprayed MEH-PPV/ZnO Nanorods Layers F.A. Mahmoud, A.B. Shehata, H. Mohamed and W. Magdy	489
Dimensional Analysis of Grid Pattern on a Nematic Liquid Crystal D. Wahyuni, I.R. Kusumawardany, S. Hartini and Y. Yusuf	493
Structural, Chemical Composition and Optical Properties of CdTe Fabricated by Vacuum Evaporation Technique Ariswan	497
The Formulation of Phonon as the Result of Second Quantization of Crystalline Lattice Vibration Using Wave Functional Method A. Hermanto.....	502
Synthesis of Tungsten Oxide (WO₃) Film on Glass Substrate Using Aqueous Based Solution Spray Deposition Method H. Widiyandari, I. Firdaus, A. Purwanto and V.G. Slamet.....	506
Effect of Oxygen Plasma on the Optical Properties of Monolayer Graphene I. Santoso, R.S. Singh, P.K. Gogoi, T.C. Asmara, D.C. Wei, W. Chen, A.T.S. Wee, V.M. Pereira and A. Rusydi	510

Chapter 8: Composites, Ceramics, and Alloys

The Influence of Sandblasting and Electropolishing on the Surface Hardness of AISI 316L Stainless Steel Suyitno and Ishak.....	517
Ground Shear Strain and Rate of Erosion in the Coastal Area of North Bengkulu, Indonesia M. Farid, K. Sri Brotopuspito, Wahyudi, Sunarto and W. Suryanto	521
Preparation and Characterization of Magnetite-Silica Nano-Composite as Adsorbents for Removal of Methylene Blue Dyes from Environmental Water Samples A. Fisli, S. Yusuf, Ridwan, Y.K. Krisnandi and J. Gunlazuardi.....	525

Development of Hydrocracking Catalyst Support from Kaolin of Indonesian Origin E.S. Rahayu, T.W. Samadhi, Subagjo and M.L. Gunawan.....	532
Adsorption Mechanism of Carbon Monoxide on PtRu and PtRuMo Surfaces in the Density Functional Theory Perspective W. Tri Cahyanto.....	537
ZnO-SiO₂/Laponite Photocatalyst: Kinetic Study on Photocatalytic Decolorization of Methylene Blue I. Fatimah and N.N. Yuyun.....	541
Hydrothermal Synthesis and Visible-Light-Driven Photocatalytic Activity of Allophane – Wakefieldite-(Ce) Composite M. Hojamberdiev, Y. Makinose, K. Katsumata, T. Isobe, N. Matsushita and K. Okada	545
Study of Internal Response of Epoxy due to Compressive Load via Experiment and Simulation Using Abaqus FEA Software I.D. Aditya, Widayani, S. Viridi and S.N. Khotimah.....	549
Development of Geopolymer Utilizing Inorganic Waste Materials T.W. Samadhi, P.P. Pratama and N. Muan	553
High Compressive Strength of Palm Oil Empty Fruit Bunches (<i>Elaeis guineensis</i>) Composites I. Sriyanti, L. Agustina, I. Selviana and L. Marlina	557
Improving the Physico-Mechanical Properties of Eco-Friendly Composite Made from Bamboo R. Widyorini, A. Puspa Yudha, R. Isnain, A. Awaluddin, T. Agus Prayitno, A. Ngadianto and K. Umemura.....	562
Properties of the Treated Kenaf/Polypropylene (PP) Composites H. Sosiati, Supatmi, D.A. Wijayanti, R. Widyorini and Soekrisno	566
Improving Mechanical Properties of Ceramic Composites by Harmonic Microstructure Control L. Anggraini, R. Yamamoto, K. Hagi, H. Fujiwara and K. Ameyama	570
Application of Carbon Fiber-Based Composite for Electric Vehicle M. Anwar, I.C. Sukmaji, W.R. Wijang and K. Diharjo	574
Coating Steel with Nanosilica by Pulsed Direct Current Electrophoresis for Corrosion Protection S.N.M.I. Putri and H. Setyawan.....	578
<i>In Situ</i> Al/Al₂O₃ Composite Coating on Steel Substrate Prepared by Mechanical Alloying at High Temperature A.S. Wismogroho and W.B. Widayatno	582
Nano-Micro Characterization of NiCoCrAl Coating on Carbon Steel Substrate S. Eni, K. Zaini, Y.M. Wang, N. Hashimoto, S. Hayashi and S. Ohnuki	586
Influence of Sintering Temperature on the Translucency of Sintered Zirconia by Cold Isostatic Pressing C.H. Chin, A. Muchtar, N.F. Amat, M.J. Ghazali and N. Yahaya.....	591
The Phenomenon of Pitting Corrosion Attack on the Milled Aluminium Alloy Al 2618 Plate during Surface Preparation through Sulphuric Acid Anodising H. Subawi and Sutarno.....	596
Study of Laser Cladding of Stellite 6 on Nickel Superalloy Substrate with Two Different Energy Inputs A. Kusmoko, D. Dunne, H.J. Li and D. Nolan	600
Interdiffusion of Elements in Aluminum 2024 Clad during Reheat Treatment Process at 495°C E. Basuki, Sutarno and Samuel	605

Boron Carbide B₂C and B₈C₁₈ Synthesized Using Boric Acid-Glucose and Boric Acid-Active Carbon at Low Temperature without Coreductor Materials M.C.F. Toana and B. Soegijono.....	609
Influence of Oxygen on Microstructures of Ti-Mo-Cr Alloy J. Syarif, E. Kurniawan, M.R. Rasani, Z. Sajuri, M.Z. Omar and S. Harjanto	613
Effect of Copper Addition on the High Temperature Oxidation of Zirconium Alloy ZrNbMoGe for Advanced Reactor Fuel Cladding Material B. Bandriyana, D.H. Prajitno and A. Dimiyati.....	617
Fractographic Analysis of 5052 Al-Mg Alloys Processed by Equal Channel Angular Pressing E. Mabururi and I.N.P.A. Gede.....	621
Fatigue and Mechanical Properties of Aluminium-Copper Bi-Metal Tubes Z. Sajuri, A. Baghdadi, M.F. Mahmud and J. Syarif	626

Chapter 9: Measurement and Characterization Techniques

Determination of Band Gap Energy of Semiconductor in Homojunction Structure Devices by Using Customized Microcontroller Based Apparatus K. Triyana, S. Ramadhan, A.M.I. Barata, Chotimah and Harsojo.....	633
Macrotexture Study of Non- and Sintered Pure Nb and Nb₃Sn Using Orientation Distribution Function K. Aniswatin, D.D. Risanti and A.W. Pramono.....	638
Modeling of Repeated Rolling Contact on Rough Surface: Surface Topographical Change R. Ismail, E. Saputra, M. Tauviqirrahman, J. Jamari and D.J. Schipper.....	642
Neutron Diffraction Measurements on Dissimilar Metal Weld of Cu-Al Obtained by Friction Stir Welding Method T.H. Priyanto, Bharoto, R. Muslih and H. Mugirahardjo.....	646
Testing of Materials for Heat and Moisture Transport V. Dvořák, P. Novotny and T. Vít	650
Simultaneous Calibration for MEMS Gyroscopes of the Rocket IMU Wahyudi, A. Susanto, W. Widada and S.P. Hadi	656
Quantitative Bump Height Analysis in ENIG Using Design of Experiment Z. Sauli, V. Retnasamy, P. Ehkan, F.A.A. Fuad and A.K.T. Yeow.....	660
Automation of Four Circle Diffractomete /Texture Diffractometer for Studies of Crystal Structure and Texture Measurements Bharoto, A. Ramadhani, N. Suparno and T.H. Priyanto	664
Celluloide Film Based Infrared Bandpass Filter for Thermography Kusminarto and U. Pratiwi.....	668
Comparison between Automatic and Semiautomatic Thresholding Method for Mammographic Density Classification S. Uyun, S. Hartati, A. Harjoko, Subanar and L. Choridah	672
Image Processing for Multiple Micro-Radiography Images A.C. Louk, G.B. Suparta and N. Hidayah.....	676
3D Micro-Radiography Imaging for Quick Assessment on Small Specimen G.A. Wiguna, G.B. Suparta and A.C. Louk.....	681
Effect of EDTA and PYP as Co-Ligand of Radiolabeled Nanomaterial M41S-NH₂ for Radiosynovectomy I. Daruwati, M.P. Christina, W.W. Perdana, N.W. Hakiki and N.K. Oekar	687

Weld Defect Classification in Radiographic Film Using Statistical Texture and Support Vector Machine	
Muhtadan, R. Hidayat, Widyawan and F. Amhar	695
Investigation of Moisture in Coal Using Electrical Capacitance Volume Tomography	
I. Maulana, D. Haryono, W.P. Taruno, M. Al Huda, M.R. Baidillah and R.I. Sulaiman	701
Design and Fabrication of Wear Testing Machine for a Fishing Net-Weaving Machine Component	
N. Intanon, C. Saikaew and P. Srisattayakul.....	706
High Performance Current-Voltage Characterization System for High Resistance Materials	
M.M. Munir, Y. Supriadani, M. Budiman and Khairurrijal.....	710
Online Monitoring of Copper Leaching Process Heterogeneity Using Electrical Capacitance Volume Tomography	
D. Haryono, H. Nugraha, W.P. Taruno, M.R. Baidillah, R.I. Sulaiman and M. Al Huda	714
High Sensitivity Fluxgate Sensor for Detection of AC Magnetic Field: Equipment for Characterization of Magnetic Material in Subsurface	
W. Indrasari, M. Djamal, W. Srigutomo and N. Hadziqoh.....	718
Flaw Detection in Welded Metal Using Magnetic Induction Tomography	
D. Sutisna, S. Ullum, W.P. Taruno, A.A.S. Iman, M.R. Baidillah, M. Al Huda, R.I. Sulaiman and D. Haryono	722
A New Type of Planar Chamber for High Frequency Ozone Generator System	
M. Facta, Z. Salam and Z. Buntat	726
Keyword Index	731
Author Index	739

Treatment of Coal Stockpile Wastewater by Electrocoagulation Using Aluminum Electrodes

Rusdianasari^{1, a}, Yohandri Bow^{2, b} and Ahmad Taqwa^{3, c}

^{1,2}Department of Chemical Engineering, State Polytechnic of Sriwijaya, Palembang, Indonesia

³Department of Electrical Engineering, Sate polytechnic of Sriwijaya, Palembang, Indonesia

^adiana_vsi@yahoo.com, ^bandre_bow@yahoo.com, ^ca_taqwa@yahoo.com

Keywords: electrocoagulation, aluminum electrode, coal stockpile wastewater

Abstract. The performance of electrocoagulation using aluminum electrodes for the removal total suspended solid and heavy metals from actual coal stockpile wastewater was studied. In a batch electrochemical cell experimental setup, two monopolar aluminum (Al) plate were used as electrodes (anode and cathode). The effects of relevant coal stockpile wastewater characteristics such as pH and total suspended solid (TSS), and important process variables such as current density and operating time on heavy metals removal efficiencies have been explored. Preliminary results show that the electrocoagulation process is able to enhance the removal of total suspended solid and heavy metal contents. The batch experiment results showed that the high heavy metals contained coal stockpile wastewater can be effectively treated using electrocoagulation. The overall heavy metals removal efficiencies have been obtained at 89.7% for ferrous and 94.6% for manganese, respectively. The removal rates of those elements were increase with operating time. Therefore, electrocoagulation technique to removal high content of heavy metal and TSS from coal stockpile wastewater is found effective and environmental friendly.

Introduction

Electrocoagulation (EC) is becoming a popular process to be used for wastewater treatment. The reuse of wastewater has become an absolute necessity. Demands to the cleaning industrial and domestic wastewater to avoid environmental pollution and especially contamination of pure water resource are becoming national and international issues. Innovative, cheap and effective methods of purifying and cleaning wastewater before discharging into any other water system are needed. EC is not a new technology [1]. EC due to some advantages over chemical coagulation is becoming a popular process to be used for wastewater treatment.

The electrocoagulation is simple and efficient method for the treatment of many water and wastewaters. It has not been widely accepted because of high initial capital costs as compared to other treatment technologies. In recent years, many investigations have been especially focused on the use of EC owing to the increase in environmental restrictions on effluent wastewater [2-3].

The use of electrocoagulation for the treatment of wastewater has been reported by various authors, and several differences were found in comparison to the chemical coagulation process. A literature survey indicates that EC is in efficient treatment process for different waste, e.g. soluble oils, liquid from the food, textile industries, or cellulose and effluents from the paper industry [4-5]. Electrocoagulation is an effective process for the destabilisation of finely dispersed particles by removing hydrocarbons, greases, suspended solids and heavy metals from different types of wastewater [6-7]. EC has been proposed in recent years as an effective method to treat various wastewaters such as: landfill leachate, saline wastewater, laundry wastewater, and chemical mechanical polishing wastewater [8].

Aluminum or iron were usually used as electrode and their cations are generated by dissolution of sacrificial anodes upon the application of a direct current [3, 5, 7]. Electrocoagulation technique for treatment of wastewater samples have been conducted on a laboratory scale and good removal of COD, color, turbidity, and dissolve solids at varying opening conditions have been obtained [3, 4, 8].

Experimental

This study is to investigate the effect of electrocoagulation process. This research is mainly focused on the capability of EC technology to improve wastewater quality, such as to increase removal efficiencies of TSS and heavy metals (ferrous and manganese).

Coal stockpile wastewater samples. Coal stockpile wastewater was obtained from the coal stockpile which located at Muara Telang, Banyuasin District, South Sumatera Province, Indonesia. The composition of wastewater then characterized to identify the total suspended solids, ferrous and manganese metals contents.

Experimental device. The batch experimental setup is schematically shown in Fig. 1. The electrochemical unit consists of an electrocoagulation cell, a D.C power supply and the electrodes (aluminum). There are two monopolar electrodes having same dimension (100 mm x 100 mm x 2 mm) as an anode and a cathode which spacing of 20 mm. In order to maintain an unchanged composition and avoid the association of the flocs in the solution, the stirrer was turned on and set at 100 rpm. All the electrodes were washed with dilute HCl before every experiments conducted. Every experiment was performed at the room temperature [9].

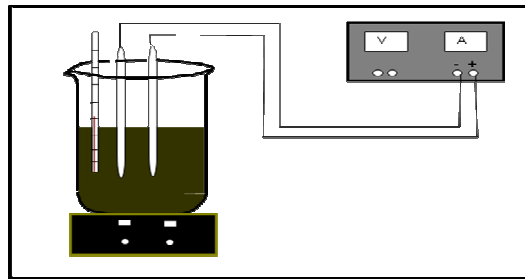


Fig.1 Schematic diagram of experimental setup

Experiment procedure. The experiments were carried out in a batch mode. For each experiment, a coal stockpile wastewater sample of 500 ml was collected in the electrocoagulation cell with two electrodes dipped into the sample. Five different of high current densities; 200 A/m², 400 A/m², 600 A/m², 800 A/m² and 1000 A/m² were applied. In each current density applied, operating time of 60, 75, 90, 105, 120 min were used. After the experiment, the treated sample was then kept undisturbed for 15 min in order to allow the flocs to settle. Subsequently, after settling the sample of supernatant was collected to perform the analysis of pH, TSS, and metal contents of iron and manganese.

Result and discussion

Characteristic of coal stockpile wastewater. Table 1 shown the characteristic of the coal stockpile wastewater sample used before the treatment.

Table 1. Characteristic of coal stockpile wastewater

Parameter	Value	Threshold standard*
pH	4.8	6-9
TSS (mg/L)	324	200
Fe (mg/L)	7.86	7
Mn (mg/L)	6.44	4

* South Sumatra Governor Regulation No.8 of 2012

Effect of current density. In all the electrocoagulation process, current density is the most important parameter in controlling the reaction rate. Rising current density resulted to an increase in the removal efficiency of TSS, metal contents of Fe and Mn. Fig. 2 shows the removal efficiency of TSS, metal content of Fe and Mn against current density applied to the aluminum electrodes in the electrocoagulation process. When the current density increases, the efficiency of ion production in

anode and cathode also increase, leading to the floc production increment. So that, 94.6%, 89.7% and 76.7% of Mn, Fe and TSS percentage of removal was obtained by using 1000 A/m^2 during 120 minutes of electrocoagulation process compared to the 53.7%, 59.1% and 38.6% of Mn, Fe and TSS respectively by using only 200 A/m^2 . The optimum of current density of 1000 A/m^2 was used for this treatment in 120 minutes. Theoretically, based on Faraday's law, operating time effects the amount of released electrode in a system with aluminum electrodes and determines the amount of produced Al^{3+} from this electrodes [11]. EC process includes two steps, destabilization and accumulation. The first step is usually short, and the second one is relatively long. With increase in operating time, both energy and electrode consumption increase and this shows that operating time is very important parameter due to affecting the cost effectiveness of EC process in polluted waters [12].

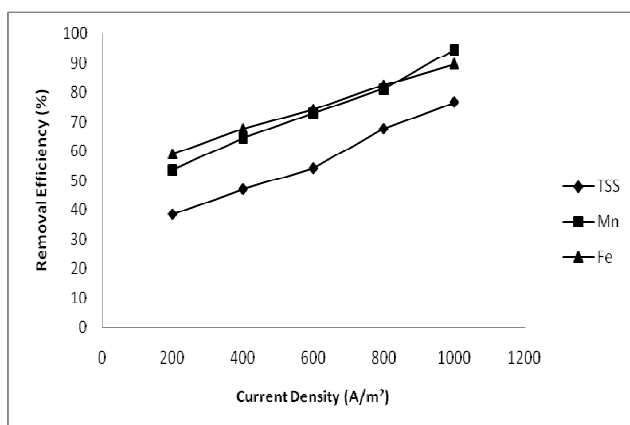


Fig. 2 Effect of current density on removal efficiency of Mn, Fe and TSS

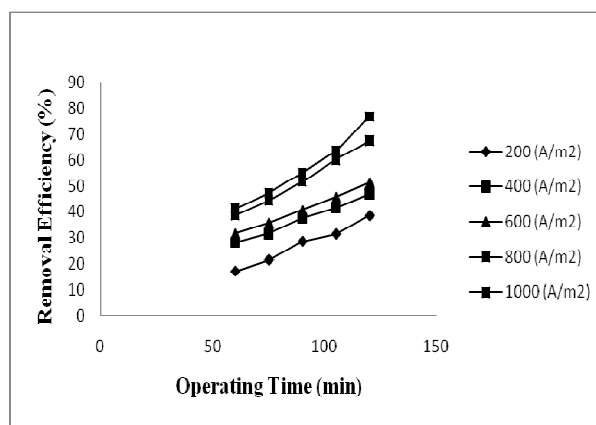


Fig.3 Effect of operating time on TSS

Effect of operating time. In the presence study, as it can be seen from Fig. 3, 4, and 5, more than 50% of wastewater quality parameters were removed in the first minutes (only 60 min), especially for current density 1000 A/m^2 , while in later minutes, the percentage of removal was low. Furthermore, as the operating time was increased, comparable increases in the pollutants removal rate were observed for all current densities. On the other hand, for a given time, the removal efficiency increasing significantly with an increase in current density.

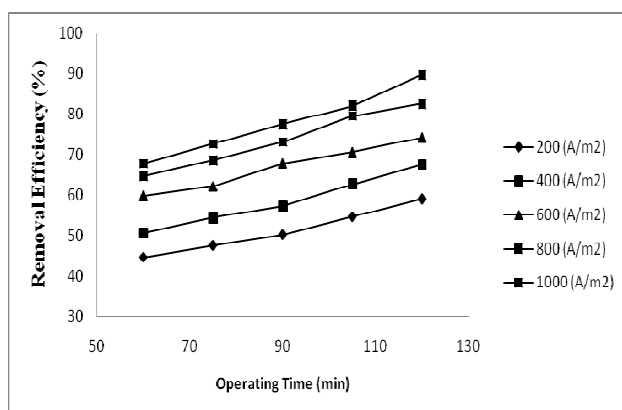


Fig. 4 Effect of operating time on Fe metal

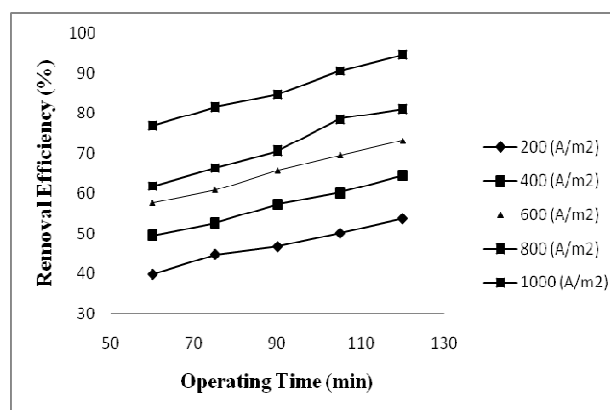


Fig. 5 Effect of operating time on Mn metal

As an example, after 120 min operating time (Fig. 5), it can be seen that 53.7%, 64.6%, 73.1%, 81.2%, and 94.6% of Mn were removed for applied current density of 200, 400, 600, 800, and 1000 A/m^2 , respectively. This describes the fact that at high current, the amount of oxidized metal increased, resulting in a greater amount of precipitate for the removal of pollutants. Similarly trends were observed for other quality parameters of coal stockpile wastewater.

Conclusion

Batch electrocoagulation studies were performed to evaluate the influence of various experimental parameters such as applied current density and operating time on the removal of pollutant from coal stockpile wastewater. The results of this study have shown the applicability of electrocoagulation in the treatment of real coal stockpile wastewater. The treatment rate was shown to increase upon increasing the applied current density and operating time. The highest current density the quickest treatment with an effective reduction of TSS, Fe and Mn concentration.

References

- [1] Holt, P.K., Barton, G.W., and Mitchell, C.A, The Future for Electrocoagulation as Localised Water Treatment Technology, *Chemosphere*. 59 (2005) 355-367.
- [2] Mollah, M. Y. A., Schennach, R., Parga, J. R., and Coker, D. L, Electrocoagulation (EC) – Science and Application, *J. Hazardous Materials*. B84 (2001) 29-41.
- [3] Kobya, M., Can, O. T., and Bayramoglu, M, Treatment of Textile Wastewaters by Electrocoagulation using Iron and Aluminum Electrodes, *J. Hazardous materials*. B100 (2003) 163-178.
- [4] Calvo, L.S., Leclerc, J.P., Tnguy, G., Cames, M. C., Paternotte, G., Valentin, G., Rostan, A., and Lapique, F, An Electrocoagulation Unit for The Purification of Soluble Oil Wastes of High COD. *Env. Progress*. 22 (2003) 57-65.
- [5] Carmona, M., Khemis, M., Leclerc, J.P., and Lapique, F, A Simple Model to predict The Removal of Oil Suspensions from Water using The Electrocoagulation Technique, *Chemical Engineering Sci*. 61 (2006) 1237-1246.
- [6] Kumar, P. R., Chaudhar, S., Khilar, K., and Mahajan, C., Removal of Arsenic from Water by Electrocoagulation. *Chemosphere*. 55 (2003) 1245-1252.
- [7] Larue, O., Vorobiev, E., Vu, C., and Durand, B, Electrocoagulation and Coagulation by iron of latex particles in Aquous Suspensions. *Separation and Purification Technology*. 31 (2003) 177-192.
- [8] Can, O. T., Kobya, M., Demirbas, E., and Bayramoglu, M., Treatment of The textile wastewater by Combined Electrocoagulation. *Chemosphere*. 62 (2006) 181-187.
- [9] Nasrullah, Mohd., Ikhveer, S., and A. Wahid, Zularisam, Treatment of Sewage by Electrocoagulation and the Effect of High Current Density. *Energy and Environmental Engineering J*. 1 (2012) 27-31.
- [10] N. Drouiche, S. Aoudj, M. Hecini, N. Ghaffour, H. Lounici, and N. Mameri, Study on the Treatment of Photovoltaic Wastewater Using Electrocoagulation: Fluoride Removal with Aluminum Electrode-Characteristic of Product. *J. Hazardous Materials*. 169 (2009) 65-69.
- [11] M. Tir and N. M. Mostefa. Optimization of Oil Removal from Oily Wastewater by Electrocoagulation using Response Surface Method. *J. Hazardous Materials*. 158 (2008) 107-115.